Asynchronous Grid Connections Providing Fast-Frequency Response: System Integration Study

Felix Wald *Student Member, IEEE*, Amir Sajadi *Senior Member, IEEE*, Barry Mather *Senior Member, IEEE*, and Giovanni De Carne *Senior Member, IEEE*

***Abstract*—This paper presents an integration study for the recent power electronic-based fast-frequency response technology, "asynchronous grid connection" which operates as an aggregator for behind-the-meter resources and distributed generators. Both technical feasibility and techno-economic viability studies are presented. The fast-frequency response characteristics, validated against Power Hardware-in-the-Loop experiments, are integrated into an IEEE 9-bus system in DigSilent PowerFactory for system-level dynamic analysis. It demonstrates that droop-based control enhancements to local distributed generators allow their aggregation to provide grid-supporting functionalities and participate in the ancillary service markets. To this end, a long-term simulation embedding the system within the ancillary service market framework of PJM has been performed. The fast-frequency response regulation is subsequently used to calculate the potential revenue and project the results on a 15-year investment horizon. Finally, the techno-economic analysis provides recommendations for enhancements to access the full potential of distributed generators on a technical and regulatory level.**

***Index Terms*—Ancillary services, Asynchronous grid, Inverter-based resources, Power system dynamics, Renewable energy sources**

I. Introduction

THE transition towards Renewable Energy Sources (RESs) is crucial, as the International Renewable Energy Agency (IRENA) advocates for a 91% share in electricity generation by 2050 [1], [2]. This shift presents new challenges, particularly in maintaining frequency stability, historically managed by synchronous generators [3], [4]. The replacement of fossil fuel-based plants is not only necessary to meet the emission targets but also economically viable, given the increasing cost competitiveness of RESs [5]. Of the technological barriers to realize this transition, this paper addresses the challenge of providing reliable and efficient Fast-Frequency Response (FFR) services [6]. Although regional system operators may recognize this service under different market terms, rules, and mechanisms, for ease of reference, in the remainder of this text it is referred to as FFR. This applies when the service is delivered within 10 seconds of an event or contingency in order to participate in the respective service framework and subsequently become entitled to compensation.

Felix Wald and Giovanni De Carne are with the Institute for Technical Physics at Karlsruhe Institute of Technology, Karlsruhe, Germany (e-mail: felix.wald@kit.edu).

Amir Sajadi is with the University of Colorado Boulder, Boulder, CO 80309, USA, and the Power Systems Engineering Center at the National Renewable Energy Laboratory, Golden, CO 80401, USA.

Barry Mather is with the Power Systems Engineering Center at the National Renewable Energy Laboratory, Golden, CO 80401, USA.

In the past two decades, various technologies have emerged, based on controllable power electronics, as tangible solutions for providing such capabilities; specifically, converter-interfaced RESs have demonstrated significant advantages [4]. Implementing FFR through RESs requires minimal control modifications, such as embedded droop characteristics during frequency events, though this may impact economic returns through power output reductions. Moreover, support during under-frequency events necessitates continuous suboptimal operation of RESs, significantly affecting economic viability [7].

Among the feasible solutions for FFR services, the use of low density, behind meter resources to support bulk power systems is gaining popularity and the utilities continue to implement and launch Demand Side Response (DSR) programs [8]. Promising control strategies in the field utilize the control margins of refrigerator fleets, selectively disconnect household appliances during emergencies, or exploit load sensitivities for adaptive power set point changes [9]–[11]. This requires a well-developed infrastructure for direct integration into a hierarchical control structure, or a sufficiently accurate network model for indirect control purposes [12]–[15]. Moreover, while the use of Vehicle-to-Grid offers additional storage capacity, it is at risk of low acceptance by the end user due to accelerated battery degradation [7]. A significant impediment to the extensive adoption of DSR is that a large number of devices must cooperate to provide a sufficient magnitude of power and allow participation in ancillary markets.

While Virtual Power Plants (VPPs) offer promising opportunities for distributed resource cooperation and subsequent participation in energy markets [16]–[18], several challenges remain. For extended time horizons, decision tree-aided load regulation successfully mitigates potential over-frequency events [19]. Recent attempts to aggregate a diverse set of participating units into simplified generic models have reduced the impact of varying latencies for frequency contingency services [20]. Nevertheless, communication constraints continue to pose challenges for VPPs in FFR applications, requiring low latency (<500ms) while executing complex control algorithms that include non-transparent black-box models and robust optimization [21]. This is precisely where the recently developed concept of the power electronic-based system called Asynchronous Grid (ASG) can improve latencies and reduce complexity by acting as a physical aggregator of distributed resources [22]. Effectively exploiting existing Distributed Generation (DG) units based on their local control objectives and responses without the need for additional communication

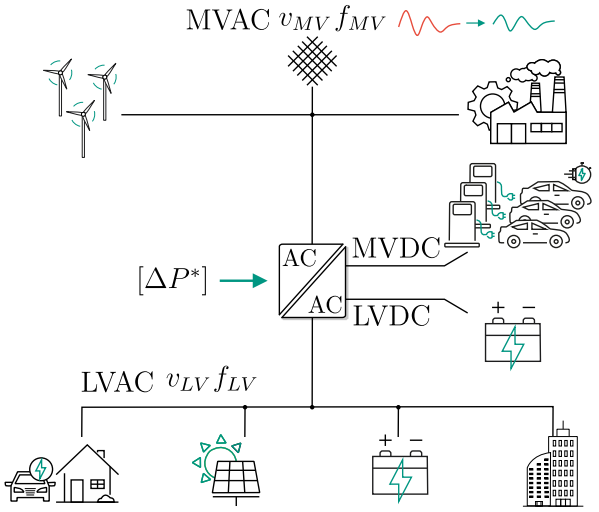

Fig. 1: Conceptual visualization for the asynchronous grid introduction.

infrastructure. Staying in the power plant analogy, the ASG essentially operates an *aggregated* power plant, instead of a *virtual* power plant. A schematic illustration of this concept is presented in Fig. 1 and explained as follows. In this technology, an asynchronous grid connection is established by the AC/AC block in the center of the figure, representing any power electronic system capable of that type of connection, e.g., *Three-Stage Solid-State Transformer*, *AC-AC Direct Matrix Converter* or a *Back-to-Back Converter* in series with a Line-frequency Transformer (LFT). Recent research has shown that the idea of creating an asynchronous cluster within a grid is technically feasible, as validated by experimental Power Hardware-in-the-Loop (PHIL) testing [22], [23]. Detailed information on design parameters and power electronics associated with this technology are available in a previous study where a prototype was tested and validated [22].

This paper integrates a Solid-State Transformer (SST)-like system as FFR-enhancing device within a power system and studies its system-level impacts using computer simulation. First, a system-level representation of the technology is developed using experimental measurements from PHIL tests. Then, the obtained model is integrated into an IEEE 9-bus system to conduct dynamic performance analysis in DigSilent PowerFactory [24] . This analysis offers a proof of concept for the adoption of this new technology and focuses on the assessment of the ASG's impact on power system dynamic performance. To achieve this, the behavior of the system with the FFRs-enhanced technology is then compared with that of the base case, which is simply the case without the ASG, and the results indicate an improvement in the system's dynamic performance, proportional to the capacity of the employed ASG. Subsequently, the economic implications of such concepts are examined and how they can participate in the energy markets. To this end, the financial value of the FFR service is evaluated, based on a specific market tariff and operational limits discovered during the technical assessment. For the market analysis, minor enhancements to the local control of DG units are proposed that allow their aggregation by deploying an ASG within the Eastern Interconnection/PJM. It is recognized that this enhancement introduces the mix of a North American tariff with a European connection rule for low voltage (LV) generators, and that these provisions have been designed according to the specific needs of their region. However, this amalgamation allows for the demonstration of how a different approach to FFR tariffs or the enhancement of connection rules for DG units could yield increased FFR capabilities on both sides of the Atlantic, which is precisely one of the objectives of this study. Finally, the market analysis is used to form recommendations on the market environment and policy.

The contributions of this paper are threefold, and they are put forth as follows.

1) This paper evaluates the dynamic performance enhancements of ASG systems for FFR, quantifying their contribution to power system stability and support.
2) It develops a techno-economic analysis of ASG systems for FFR, building a business case by quantifying the value proposition and the revenue potential.
3) It provides a critical perspective on market structure and incentives for DG, focusing on SST and regulatory considerations to hedge investment risk.

In addition to the FFR service provision explored in this study, the physical, asynchronous aggregation, and clustering of the power system sections can yield advantages such as: intentional islanding; enabling autonomous downstream grid operation; upstream grid support, e.g., reactive power compensation and limiting fault and disturbance propagation.

The remainder of this paper is organized as follows. Section II presents a detailed explanation of the model development of the ASG system. Section III evaluates the impacts of this technology on the power system dynamic performance. Section IV develops a comprehensive analysis of the economic implications of the proposed technology. Section V presents a critical opinion about market incentives and regulations that could help mitigate investment risk. Section VI concludes and closes the paper.

II. Asynchronous Grid Response Modeling

The recently developed asynchronous grid connection technology [22] utilizes two Back-to-Back connected low-voltage converters in series with a conventional LFT. This configuration ensures sufficient power supply to a downstream grid, as shown in Fig. 1. PHIL testing of the prototype, successfully demonstrated the control of the active power flow at device level around its original operating point. This control of active power flow allowed the support of the upstream grid during frequency contingency events.

The active power flow control concept is based on a form of DSR that is mandatory for all converter-interfaced generation units newly deployed within the German power system due to the standards VDE-AR-N 4110 and 4105 for medium voltage (MV) and LV respectively [25], [26]. The standard requires the implementation of a droop characteristic, essentially creating an active power-to-frequency sensitivity, defined as the

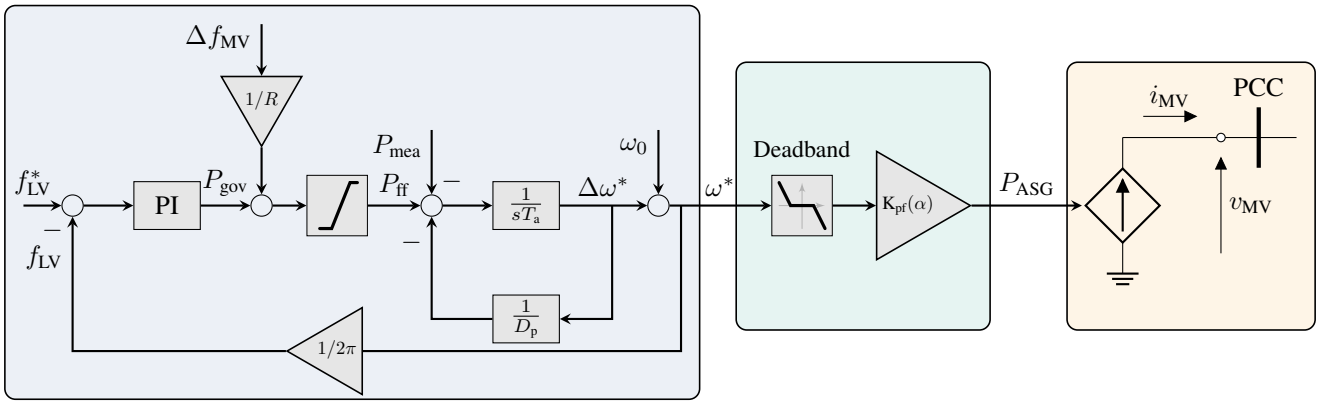

Fig. 2: ASG model, including controller and converter average model, implemented within an RMS simulation in DigSilent Power Factory.

variation of active power with respect to a frequency change, as follows:

$$\text{K}_{\text{pf}} = \frac{\Delta P/P_0}{\Delta f/f_0} \tag{1}$$

where K_{pf} is the sensitivity of the units' active power to frequency, f is the frequency, P is the active power, f_0 is the nominal frequency, and P_0 is the rated active power. Following the above-mentioned German standards, if the frequency of a LV grid is outside of a [49.8, 50.2] Hz deadband, the active power of a generation unit must follow the frequency with a sensitivity of $\text{K}_{\text{pf}} = -20$ for the generation units and $\text{K}_{\text{pf}} = -20$ (resp. $\text{K}_{\text{pf}} = 50$) for an energy storage unit for over-frequency (resp. under-frequency). The asynchronous grid connection then utilizes the flexibility to adjust the downstream frequency (f_{LV}) within the boundaries of the grid code and therefore enforces an active power response from the downstream units. Using this mechanism, the active power flow can be controlled around the current operating point which is an effective lever for the provision of a fast-frequency response service.

For the following system integration analysis, an abstracted model of the ASG technology was developed that captures its non-linear properties and matches the behavior observed in PHIL testing. Focusing on FFR applications, the model represents active power behavior and control processes over several seconds while omitting less significant dynamics. The mathematical model development is detailed below and validated against experimental data to ensure accuracy.

A. Mathematical Model

A reduced-order representation of the control system that operates the proposed ASG technology is visualized by the block diagram shown in Fig. 2. The governing principles of this control system and their mathematical models are explained throughout this subsection.

A set of equations can adequately describe the ASG model as follows:

$$\text{G}_{\text{gov}}(s) \triangleq P_{\text{gov}} = (f^*_{\text{LV}} - f_{\text{LV}}) \left(\text{K}_{\text{pgov}} + \frac{\text{K}_{\text{igov}}}{s} \right) \tag{2}$$

$$\text{G}_{\text{prop}}(s) \triangleq P_{\text{ff}} = \frac{1}{R} \cdot \Delta f_{\text{MV}} + P_{\text{gov}} \tag{3}$$

$$\text{G}_{\text{vsm}}(s) \triangleq \omega^* = \frac{1}{sT_{\text{a}}} \left(P_{\text{ff}} - P_{\text{mea}} - \frac{1}{D_{\text{p}}} \Delta\omega \right) \tag{4}$$

subject to:

$$-\text{P}_{\text{lim}} \leq \text{P}_{\text{ff}} \leq \text{P}_{\text{lim}} \tag{5}$$

In Eq. (2), $\text{G}_{\text{gov}}(\text{s})$ represents the transfer function of the governor, which is a PI controller with the proportional gain of K_{pgov} and the integral gain of K_{igov}. Its goal is to steer the frequency of the downstream LV grid (Δf_{LV}) back to its nominal value by adjusting the active power set point (P_{gov}). The active power set point P_{gov} is subsequently altered in Eq. (2), by a feed-forward summation of the amplified MV frequency deviation (Δf_{MV}) as in Eq. (3), where R is the droop coefficient used to amplify that deviation. The downstream LV grid-forming controller uses a Virtual Synchronous Machine (VSM) to regulate the phase angle of the supplied voltage. Multiple factors influenced the choice of the controller. Among others the ability to operate in grid-forming mode as well as grid-following and the flexibility to regain the nominal frequency value in a quick and smooth manner, lead to a combination of VSM and PI governor controller. The transfer function of the VSM Eq. (4), is based on a first-order swing equation proposed by Sakimoto et al. in 2011 [27]. It consists of the damping coefficient D_{p} and has a time constant T_{a} that represents the virtual moment of inertia. The input variables are the measured electric active power P_{mea} and the enhanced active power set point P_{ff}, with the goal of adjusting the frequency set point ω^* to achieve the desired active power flow. The active power set point is subject to the limitation expressed in Eq. (5). This is needed to ensure the LV frequency set point ω^* stays within the LV distribution grid code boundaries, 47.5-51.5 Hz [28].

The reaction of the active LV distribution grid to the frequency set point ω^* is based on a simple droop characteristic

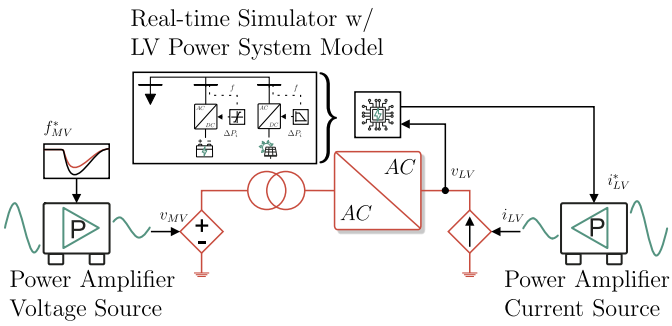

Fig. 3: Back-to-Back Converter in the double PHIL test bed.

with coefficient $\mathrm{K_{pf}}(\alpha)$, shown in Eq. (6). This factor is subject to the composition of load/generation in the LV distribution grid at that specific time, defined by α, where $\alpha \in [0, 1]$, representing 0-100% of power absorbed/injected by active units obeying the German grid codes mentioned previously.

$$\mathrm{G_{LV}} \triangleq P_{\mathrm{ASG}}(i_{\mathrm{d,q}}) = \begin{cases} \omega \cdot \mathrm{K_{pf}}(\alpha), & \text{if } |\Delta\omega| \geq 200\,\mathrm{mHz} \\ 0 & \text{otherwise} \end{cases} \tag{6}$$

subject to:

$$0 \leq \alpha \leq 1 \tag{7}$$

The different control processes described above are highlighted by colors in the block diagram shown in Fig. 2. The ASG controller with the governor, frequency propagation, and swing equation (Eqs. (2) to (4)) is located in the blue box. In the green shaded box, the calculation of the power response of the LV distribution grid droop characteristic (Eq. (6)) takes place. The LV-side calculation is followed by the set point feed-through to the electrical representation of the ASG and its connection to the power system in the yellow box. The transfer functions in Fig. 2 represent a grid-forming converter model based on a PI governor and a VSM, with the addition of a power set point adaptation based on the upstream frequency. This adaptation leads to the active power adjustment of LV DG, which is injected/absorbed by the current source in the yellow box.

As depicted in the yellow box, the upstream converter of the ASG functions as a current source due to its grid-following operation with supporting features. Calculated currents are interfaced with the interconnection point to the grid. Since active power control forms the foundation for FFR, the developed model emulates the active power of the LV distribution network interfaced by an asynchronous grid connection.

B. Model Validation - Power Hardware-in-the-Loop Testing

To ensure accuracy of the derived model, it was validated against the experimental data collected in a previous study [22]. The validation test case is based on a PHIL experiment, testing the ability of an ASG system to adjust the downstream active power set point using the frequency of voltage v_{LV}. A single line diagram of the setup is illustrated in Fig. 3, where the back-to-back converter is shown in the center, connected to two power amplifiers, representing the

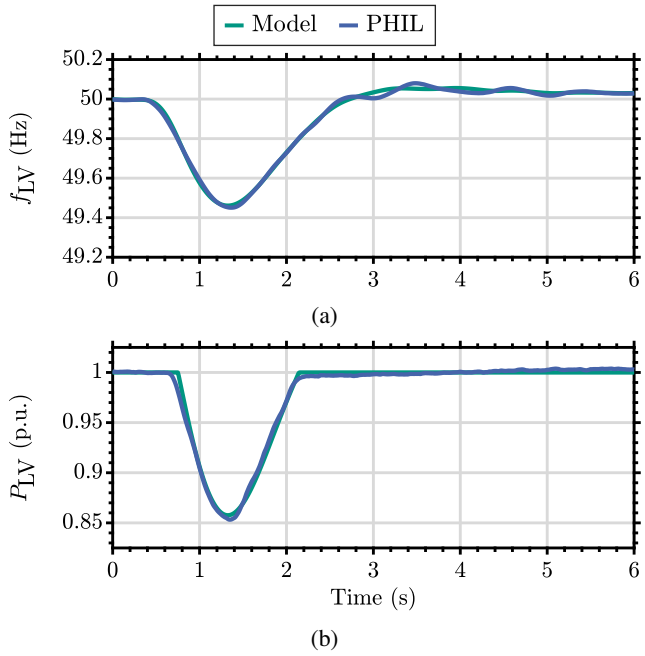

Fig. 4: The green line in a) shows the low-voltage frequency of the developed model, while the blue line represents experimental benchmark acquired in the PHIL experiment. As a result of the frequency the active power flow adaptation is illustrated in b), using the same color code.

medium and low voltage power systems, respectively. The amplifiers are controlled by a central *Real-time Simulator* executing both a single machine MV power system model and the LV distribution grid model, using a 24 μs time step. In Fig. 3, the MV power system is represented as a voltage source (v_{MV}), while the primary (left) side of the ASG directly connected to the medium voltage side is acting as a grid-following active front-end converter, which can be model as a current source (analog to the yellow section in Fig. 2). This current source behavior is responsible for supplying the secondary side LV converter with sufficient power. The secondary side converter is thus operating as grid-forming node. It is supplying the LV distribution grid with the needed power and can be modeled as a voltage source connected to the emulated LV grid represented by a current source (i_{LV}). The parameters used for this validation are based on the parameters used in a previous hardware-related study. The Root-Means-Square (RMS) deviation is used as the metric to quantify the precision of the analytical model and the data from the PHIL tests. The model fitting was conducted by minimizing the following objective function:

$$\mathrm{RMSD} = \sqrt{\frac{1}{n}\sum_{i=1}^{n}\left(y_{\mathrm{exp}}(t_i) - y_{\mathrm{sim}}(t_i, \mathbf{p})\right)^2} \tag{8}$$

Here, $y_{\mathrm{exp}}(t_i)$ represents the experimental data at time t_i, $y_{\mathrm{sim}}(t_i, \mathbf{p})$ represents the simulated data at time t_i given the parameter vector $\mathbf{p}$, and n is the number of data points within the specified time window. The final parameters used are given in the appendix in Table IV.

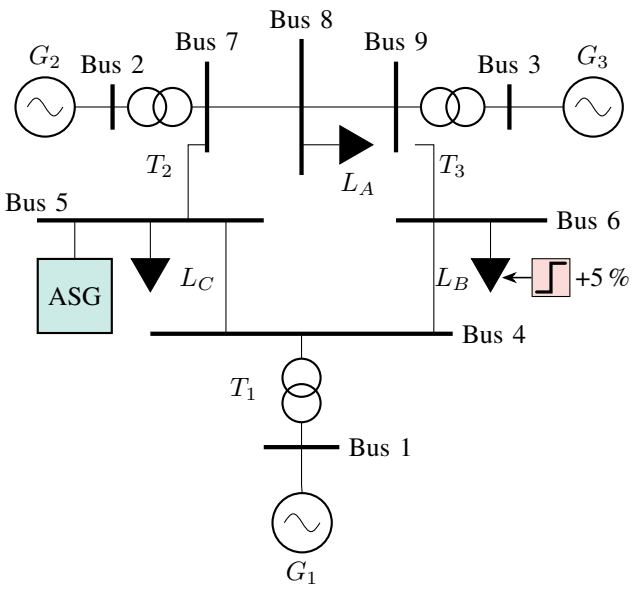

Fig. 5: Single-line diagram of the IEEE 9-bus system [24], [29].

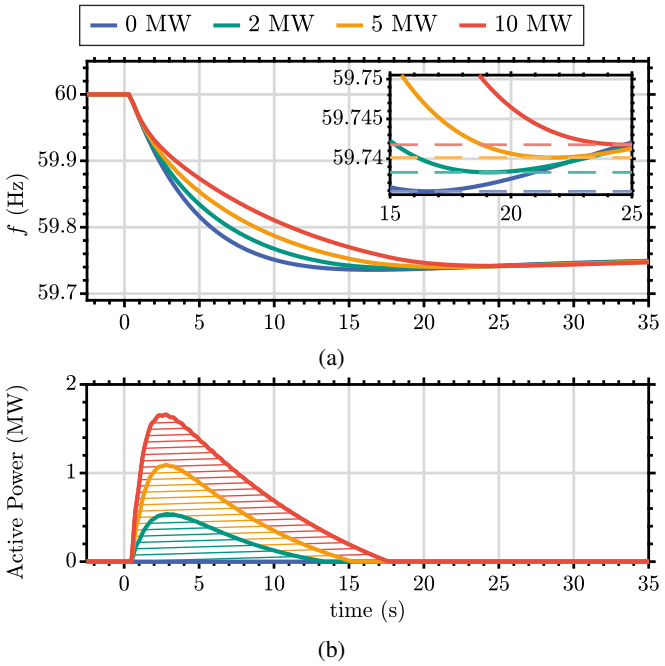

Fig. 6: Plot of the system frequency at bus 6 in a) for a frequency response of the ASG for different power ratings of the ASG, the respective active power flow shown in b).

The test event is triggered by a frequency disturbance on the MV side of the connection (f_{MV}), which causes the system to initiate the FFR. f_{LV} in Fig. 4a, represents the reaction of the downstream frequency of the developed model in green, and the actual PHIL result in blue. The RMS deviation between the model and experimental results yields a 0.027 % mean deviation during the frequency disturbance, which is small, thus, acceptable. Fig. 4b, illustrates the resulting adjustment of the active power flow due to the altered set point of the frequency f_{LV}. The RMS deviation between the active power curves yields a 0.5 % mean deviation, which is also small and acceptable. These results validate the mathematical model with sufficient accuracy to represent the proposed FFR response in system-level integration studies, which will be the subject of investigation in the subsequent section.

III. System Integration and Dynamic Analysis

This section seeks to understand the fast-frequency response capability that an asynchronous grid connection can offer and its impact on the dynamic performance and system stability when integrated within a power system. The dynamic performance analysis was conducted using the modified IEEE 9-bus benchmark power system [24], [29].

A. Computer Simulation Procedure

Implementation in DigSilent Power Factory began with initial parameter validation of the ASG. A *Static Generator* block implements the response algorithm, acting as a controllable power source capable of injecting or absorbing active power calculated by the ASG control structure shown in Fig. 2. Through an automated Python interface, the combined IEEE 9-bus system and ASG model enables iterative parameter changes and comparative analysis across different cases. Fig. 5 illustrates the single-line diagram of the 9-bus system, including the ASG and the load step used as a frequency disturbance trigger. The detailed parameters are provided in tabular form in the Appendix in Table VI. The controllable power source/sink block representing the ASG responds to system frequency dynamics by injecting or absorbing power at bus 5 (the load bus between generator 1 and generator 2). Bus 5 was chosen arbitrarily after a preliminary assessment revealed that the ASG location in this system was not a determining factor for its impact on the system's frequency response.

The analysis involved four distinct scenarios: a base case without an ASG system, and three configurations with ASG systems rated at 2 MW, 5 MW, and 10 MW respectively. Each scenario faced disturbance through a +5 % load change at Bus 6, equivalent to 4.5 MW additional load power (red shaded step block in Fig. 5). While this creates a relatively large frequency deviation exceeding 250 mHz, it effectively demonstrates the proposed concept's capabilities.

The resulting time series of the frequency at each bus is subsequently transferred to MATLAB using the Python library *MATLAB Engine*. For time-domain analysis and the subsequent economic evaluation, MATLAB and Python serve as the main tools.

B. Time-Domain Analysis

Upon system disturbance, the frequency drops due to a mismatch between generation and consumption. As shown in Fig. 6, the resulting frequency responses vary with different levels of ASG participation, with the baseline behavior (without ASG) shown in blue. Baseline measurements record

TABLE I: Comparative performance of different cases equipped with ASG with respect to the base case - the measurements are from bus 6.

P_{ASG}	Δt_{NADIR}	% to Base	RoCoF	% to Base	ΔE (kWh)
Base	16.44 s	0.00	5.2 $\times 10^{-2}$	0.0	0.00
2 MW	19.20 s	+15.78	5.0 $\times 10^{-2}$	-5.7	1.95
5 MW	21.60 s	+31.38	4.6 $\times 10^{-2}$	-12.5	10.99
10 MW	24.78 s	+50.70	4.2 $\times 10^{-2}$	-20.4	38.15

the frequency nadir at 16.44 s, while the ASG implementation delays this occurrence. Systems equipped with 2 MW, 5 MW, and 10 MW ASG reach the nadir at 19.20 s, 21.60 s, and 24.78 s respectively. Additionally, nadir frequency values improve from 59.736 Hz (baseline) to 59.738 Hz, 59.740 Hz, and 59.742 Hz with increasing ASG ratings. As evident here, and as the core functionality of the ASG suggests, its introduction aids the frequency response in the form of a delayed nadir time and marginally less frequency deviation (that is lower nadir). In addition, the Rate of Change of Frequency (RoCoF) is significantly reduced by 5.7 %, 12.5 % and 20.4 %. This frequency response support is safely attributed to the additional active power provided by the ASG, as it is the only parameter that distinguishes these cases. For a more convenient depiction of this effect, the nadir section is magnified in the top right of Fig. 6.

For comparative purposes, the response from the three cases with ASG with respect to the base case was quantified using the time it takes for the frequency to reach its nadir in seconds, Δt_{NADIR}, and its percentage change (%.) In addition, the amount of energy injected by ASG, ΔE was included. Which is the integral value of active power injection ΔP, illustrated in Fig. 6b and highlighting ΔE as the shaded area below each line. The quantitative results are shown in Table I. Comparing the time from the start of the disturbance until the nadir is reached shows that a 2 MW support system would increase the time by 15 %, with the possibility of nearly 50 % for a 10 MW support system.

C. Modal Analysis

Looking at the time-domain traces, one could reasonably argue that all cases studied have similar frequency trajectories. Herein lies the motivation for modal analysis to learn how this technology may alter dynamical modes that are excited during the frequency response as the focal point of the analysis. To this end, Prony's analysis is applied to the time-domain frequency signals recorded in the simulation [30]. Prony's method is a data-driven technique for studying dynamical systems because of its ability to estimate eigenvalues of a nonlinear system that emerge from small-signal disturbances by using a measured data sequence to fit a linear combination of complex exponential terms with damping in form of [31]:

$$f(t) = \sum_{i=1}^{N} A_i e^{\sigma_i t} \cos(\omega_i t + \phi_i) \tag{9}$$

where N is the number of terms and A_i is the amplitude, σ_i is the damping factor, ω_i is the frequency, and ϕ_i is the phase of ith term, representing the eigenvalue in the form of $\lambda_i = \sigma_i + \pm \boldsymbol{j}\omega_i$.

In this analysis, the two-term solution was sought; yielding a pair of complex conjugate roots, given that the frequency response of generators in a power system around its fundamental frequency resembles the response of second-order harmonic oscillators [4]. The outcome of the modal estimation regarding the frequency response for differing levels of support from the ASG are shown in Table II.

TABLE II: Dominant modes of the frequency response.

P_{ASG}	λ_{12}	f	ζ
Base	-0.174 $\pm$ $\boldsymbol{j}$ 0.184	0.029	68.61
2 MW	-0.178 $\pm$ $\boldsymbol{j}$ 0.162	0.026	74.01
5 MW	-0.182 $\pm$ $\boldsymbol{j}$ 0.145	0.023	78.31
10 MW	-0.186 $\pm$ $\boldsymbol{j}$ 0.127	0.020	82.55

The results yield a negative root for the oscillatory modes, which was expected for time-domain signals being all stable, in all cases considered. They show that the frequency of excited modes, denoted by f, becomes smaller proportional to the increase in contribution from the ASG. This frequency is computed as $f_i = (2\pi)^{-1}\omega_i$. The lower this frequency, the less oscillatory the response; therefore, the more desired. The higher contribution from the ASG technology also appears to increase the damping ratio of oscillatory modes, ζ. The damping ratio is a dimensionless metric that relates to the decay of system oscillations following a transient. It is computed as $\zeta_i = \frac{\sigma_i}{\sqrt{\sigma_i^2+\omega_i^2}} \times 100$ and ranges between 0 and 100; the higher the damping ratio, the better the dissipation of transients. This suggests that the additional fast power injection by the ASG technology helps eigenvalues migrate further away from the imaginary axis and simultaneously move closer to the real axis. The injection provides an additional damping-like support without changes to inertial momentum in the system. This observation is corroborated by the analysis shown in [4] for the signature characteristics of increased damping in the system.

The time-domain results and eigenvalue analysis collectively established that the use of the ASG technology can offer a positive contribution by improving frequency nadir and ROCOF. Next, the financial viability of deploying such technology under current market incentives, tariff structures, and subject to performance limitations, will be explored.

IV. Economic Evaluation

Having established technical feasibility, this section investigates the market participation potential of the ASG technology in frequency response services, focusing on revenue stream identification. This analysis explores the deployment of the ASG in North America, specifically within the Pennsylvania-New Jersey-Maryland (PJM) market. As a Regional Transmission Organization (RTO) in the Eastern Interconnection of the United States, PJM operates an electric transmission system across 13 states within the Eastern Interconnection grid. This analysis proposes an enhancement to the PJM protocols related to the DG units, following German standards,

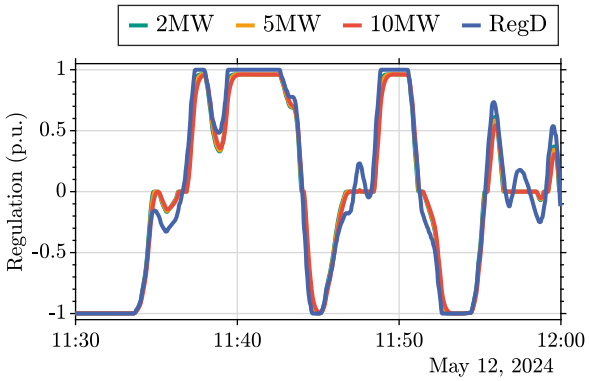

(a)

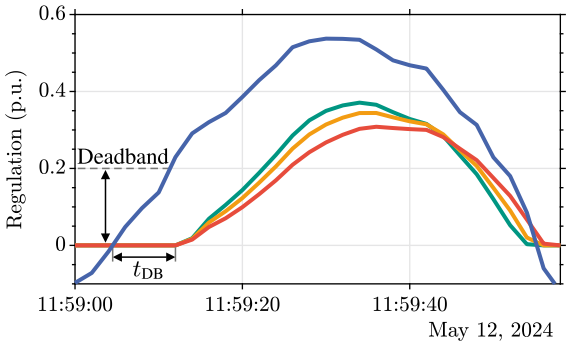

(b)

Fig. 7: The time series in a) shows 30 minutes of the regulation signal *RegD* in blue paired with the ASG regulation for different power ratings in green, yellow and red. b) is a zoomed in version of the same data, highlighting the difference between the power ratings and the impact of the deadband and ramp rate limitation.

such that newly connected DG units are required to provide active frequency response through droop characteristics, as discussed in Section II and described in Eq. (6) [25], [26].

The proposed integration of PJM-style regulation markets with German-inspired DG features would enable power electronic systems like the ASG to aggregate DG fleets physically, offering profitable frequency response services. Most notably, such an approach eliminates the need for additional communication infrastructure or complex control hierarchies typically required for aggregating dispersed DG.

A. PJM Regulation Concept - RegD/A

PJM, operates a real-time ancillary service market, in which the frequency regulation service is based on an Automatic Generation Control (AGC) concept, sending regulation signals to participating units, to help maintain a balanced system. The signals for frequency regulation are divided into two signals, *RegA* and *RegD*. *RegA* represents a low-pass filtered Area Control Error (ACE) signal for traditionally slow-acting resources. *RegD* is a high-pass filtered ACE signal designed for fast response resources, e.g. SSTs or Energy Storage Systems. In this scenario, given the fast-responding nature of the ASG, the participation in the *RegD* regulation scheme is investigated. PJM sends the signal in intervals of 2 seconds to participating systems, with normalized values of -1 to 1. This value is not directly applicable as an active power set point within the ASG controls; therefore, by rescaling it as outlined in Eq. (10) a scaled frequency set point will be generated.

$$f^*_{LVsc} = \text{rescale}(regD) \cdot f^*_{LV} \tag{10}$$

$$\mathrm{G_{gov}}(s) \triangleq P_{\text{gov}} = (f^*_{LVsc} - f_{LV}) \left(\mathrm{K_{pgov}} + \frac{\mathrm{K_{igov}}}{s} \right) \tag{11}$$

In Eq. (10) the correct adjustment of the frequency set point is ensured. This in turn provokes the respective droop control reaction within the DG units, due to the enhanced behavior introduced by the German standard VDE-AR-N 4105 [26]. To adjust f^*_{LV}, which is in per unit and is usually set to 1, the *RegD* signal is rescaled to adjust the frequency to up to $\pm$ 1 Hz. For a 60 Hz system that requires a rescaling of the *RegD* signal from $[-1\ ..\ 1]$ to $[0.935\ ..\ 1.0165]$ as in Eq. (10). The governor previously described by Eq. (2), now Eq. (11), uses the value f^*_{LVsc} as the new set point of the nominal frequency.

A 30-minute window of the simulation data is displayed in Fig. 7a, the active power adjustment is only triggered after the frequency set point is outside the 200 mHz deadband, which translates to 20 % of the allowed $\pm$ 1 Hz frequency deviation. The influence of the deadband is illustrated in the zoomed plot, in Fig. 7b, where the regulation signals react after the *RegD* signal is outside the deadband of 20 %. Additionally, this plot highlights that a power electronic system with a higher power rating might be limited by the ramp rate at which it is allowed to change its output power, thus not reaching its nominal power before the regulation decreases its demand again. This leads to a reduced overall regulation, with respect to the power rating, which will subsequently impact the potential revenue, discussed below.

B. Short-Term Revenue Forecast

PJM's frequency response service compensation follows a pay-for-performance model, aligned with FERC Order No. 755. Compensation depends not only on the volume of regulated active power but also on signal adherence precision [32]. The performance evaluation combines actual integrated power regulation (capability or mileage, $\mathrm{M_{RegD}}$) with performance score (ρ) to determine five-minute remuneration credits. A publicly available PJM excel tool yielded $\rho = 0.5$, resulting in a smaller value than the suggested default for demand response units ($\rho = 0.76$) [33]. In addition to capability and performance score, the mileage ratio β_t^M is used and defined as:

$$\beta^{\mathrm{M}}_{\mathrm{t}} = \frac{\mathrm{M_{RegD}}}{\mathrm{M_{RegA}}} \tag{12}$$

where the mileage ($\mathrm{M_{RegD}}$) is the integrated movement of the regulation control signal, as shown for *RegD* below:

$$\mathrm{M_{RegD}} = \sum_{i=1}^{N} |\mathrm{RegD}_i - \mathrm{RegD}_{i-1}| \tag{13}$$

here N=150 is the number of 2-second samples in the 5-minute evaluation window. This calculation process subse-

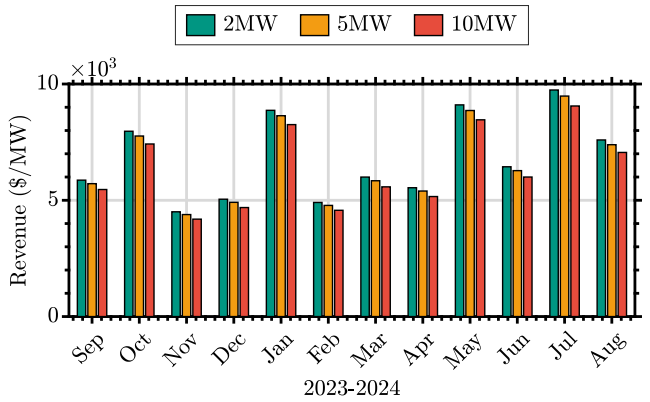

Fig. 8: Monthly revenue within PJM regulation from 09/23-08/24 for three ASG power ratings.

quently yields the regulation credit (C_{reg}) for a 5 minute window, based on the following equations:

$$C_{reg} = M_{RegD} \cdot \rho \cdot (\lambda_C + \beta_t^M \cdot \lambda_P) \tag{14}$$

with the *Regulation Capability Clearing Price* as λ_C (in \$/MW), M_{RegD} (in MW) integrated regulation within the time window and the *Regulation Performance Clearing Price* represented by λ_P (in \$/Δ MW). Both clearing prices are sourced from the historical data during the investigated time period. The database is freely accessible through PJM's open data miner interface and provides the full 5 minute resolution clearing prices [33], [34]. During the study period (09/23-08/24), λ_C ranged from 0 to 238.5\$/MW and λ_P ranged from 0 to 2.8\$/Δ MW, with average values of 2.2\$/MW and 0.08\$/Δ MW respectively. In the scenario studied, an average distributed power generation of 2, 5 and 10 MW within the downstream grid is assumed, offering its active power through the droop characteristic of Eq. (6). Using Eq. (14), the monthly revenue of an ASG system indirectly controlling downstream DG, is in the range of 4,000 - 10,000 \$/MW, as illustrated in Fig. 8. The revenue bar chart also highlights the slightly reduced revenue per MW, for a system with higher power rating due to the ramp rate limitation and subsequently a worse performance score (ρ), as mentioned above.

C. Long-Term Cash-Flow Forecast

The long-term financial evaluation of the new technology begins with calculating the Net Present Value (NPV), which serves as a primary indicator of investment profitability over the chosen 15-year horizon. The NPV uses the future cash flow (Cf) discounting its value back to the present day to ensure that all future earnings and expenses are accounted for, the calculation is based on the following formula:

$$NPV = \sum_{t=0}^{T} \frac{\mathrm{Cf}(t)}{(1+\mathrm{r})^t} \tag{15}$$

where T is the total number of periods (years) and r is the discount rate applied to the cash flows. The initial annual revenue of $\sim$ 80,000\$/MW and the operation and maintenance costs (c_{OM}) are estimated to increase with a growth rate of 6%. The c_{OM} costs are assumed to amount to an initial value of 2% of the initial investment cost I. The growth rate is subject to various economic factors within the global economy, which is why a reliable prediction into the future is impossible. The rate has therefore been chosen based on historical data and recommendations by the Inter-American Development Bank [35]. Naturally, the result is very sensitive to the growth and discount rate, the reference discount rate is aligned with the growth rate to r = 6%, which leads to a NPV for a 2 MW system of 1,016,500 \$/MW over a 15-year investment horizon, as shown in Table III. Changing r to 8%, reduces the NPV to 995,670 \$/MW, while a much bigger increase of r = 20% results in a NPV of 885,360 \$/MW. This leads to the conclusion that the investment is profitable, even for very high discount rates of up to 20%. All economic parameters for the performed analysis are listed in tabular form in the Appendix in Table V.

The second metric to be considered in the long-term analysis is the Internal Rate of Return (IRR). The IRR over a range of investment costs, as illustrated in Fig. 9a, emphasizes the economic viability of the ASG system, as in the presented scenario of DG aggregation in the PJM region. Scaling the investment cost for the ASG system in the range of 1 to 5 times the base investment cost always yields a minimum IRR value of more than 0.13. This shows that the results are reliable even for higher costs of production or material. Thus, even with investment costs five times higher, an interest rate of 13% is required to make the investment more profitable than the ASG, according to the assumptions of this study. The IRR is determined as the rate that brings the NPV equal to zero, instead of the previously predefined discount factor r. It is calculated numerically by solving the following equation:

$$0 = \sum_{t=0}^{T} \frac{\mathrm{Cf}(t)}{(1+IRR)^t} \tag{16}$$

Both previously introduced metrics are based on future cash flows, the sum of the total revenue of the simulated year (initially $\sim$80,000 \$/MW). To forecast the potential long-term revenue for the next 15 years, the rather conservative revenue growth rate of 6% is applied [35]. The yearly cash flow (Cf) is calculated by subtracting investment cost (I) and operation and maintenance cost (c_{OM}) from the annual revenue ($\Sigma C_{reg}(t)$), as in:

$$\mathrm{Cf}(t) = \Sigma \mathrm{C}_{\mathrm{reg}}(t) - \mathrm{I}(t) - \mathrm{c}_{\mathrm{OM}}(t) \tag{17}$$

c_{OM} is estimated as a percentage of the capital investment (2 %), increasing with the capital growth rate, and I is only included as a negative cash flow in the first year of the project. The resulting revenue per MW increases to up to 184,000 \$ displayed in Fig. 9b, and is used to calculate the resulting cash flow during the 15-year period. The cumulative cash flow in Fig. 9c displays the forecast for a 15-year investment period. It includes variations in the initial investment cost (I), shown in dark green, green, and light green lines. These lines represent factors of 1, 2, and 3 times the base investment cost of 137,500\$/MVA or 137.5\$/kVA. This assumes that the investor has to buy a full B2B system in addition to a traditional LFT if it is not already available. These capital costs are on the

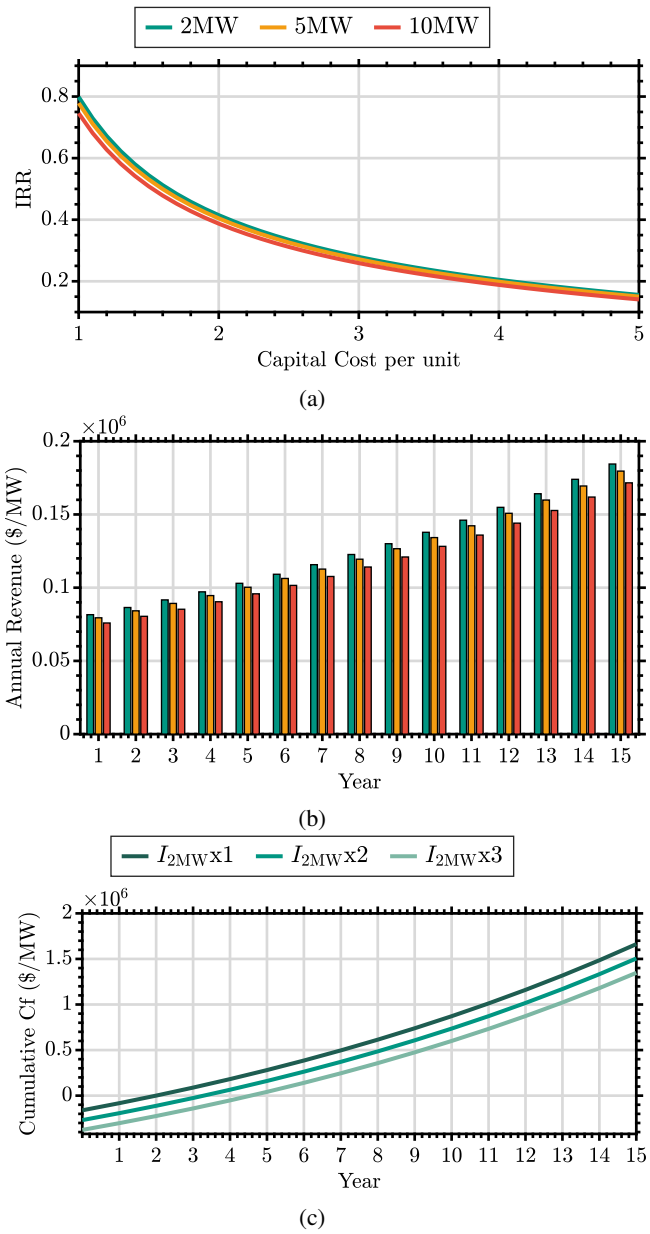

Fig. 9: The figures display the IRR for a variation of the capital cost of a Back-to-Back Converter (B2B) + LFT by a factor of 1 to 5 in a), the projected yearly revenue for a 15 year horizon based on the annual revenue in b). The top legend applies to figure a) and b) while figure c) has its own legend. c) shows the cumulative cash flow forecast for a 2 MW system and variations of the investment cost I.

conservative side, Huber and Kolar estimated the material cost for a full SST to 52$/kVA back in 2014, where the cost for power electronics decreases with their maturity [36]. Nonetheless, the exact cost figures are a result of confidential discussions within industrial and academic working groups, which is why a diverse analysis for a range of investment costs of up to 3 times the base 135$/kVA is offered. Analysis of the cumulative cash flow in Fig. 9c evidently shows that the system breaks even after at least 5 years for all the shown cases, but could break even after only 2 years.

TABLE III: IRR, NPV and Revenue for 1x Capital Cost.

P_{ASG}	IRR	NPV (per MW)	Revenue 09/23-08/24 (per MW)
$2\,MW$	0.80	1,016,500 $	81,578 $
$5\,MW$	0.78	986,220 $	79,439 $
$10\,MW$	0.75	936,090 $	75,897 $

V. Discussion and Perspective

Globally, experts agree on the need for more renewable energy facilities, leading to power systems with reduced mechanical inertia and increased frequency volatility. This shift requires enhanced transmission infrastructure to transport clean energy from remote locations to demand centers and updates to aging systems. The evolving technological landscape presents an opportunity to adopt SST-like power electronic systems in substations as alternatives or supplements to traditional transformers.

This study demonstrates the technical merits of a fast-frequency response facilitated by an aggregator based on an SST-like power electronic system [37]. Still, there remain open questions and investigations to be answered and performed, including the integration of one and/or multiple ASG systems in large and more complex power systems with high penetration levels of inverter-based resources. The main section of the study, the economic analysis, finds the ASG to be a promising, market-competitive asset and filled a long-lasting gap within the research landscape regarding the economic viability of SST-like systems, also known as energy routers or smart substations. The technical motivation for the introduction of an increased number of power electronic systems to manage the power system is extensive; one major bottleneck for system operators or private investors has always been the question of economic viability. Despite the fact that the analysis suggests the financial viability of the ASG technology, based on a combination of American and German standards and concepts, it is expected that the changing nature of the grid will naturally create a better financial environment and most importantly compatible regulatory frameworks. This is due to the likely increase of ancillary service prices within the foreseeable future due to the expected continued trend of reduced inertia and a possible reduction of the capital cost as power electronics technologies continue to mature. However, the increase in the prices of ancillary services will not be indefinite, as the FFR capacity may grow accordingly and lead to more competitive pricing. Nonetheless, recent developments show that the transformation of the power system could take a very long time (perhaps decades) to reach the worldwide emission reduction targets. Thus, it is concluded that the time scales in which a ASG system providing FFR breaks even are much shorter than the general transformation time scales of the power system. Furthermore, providing a long-term prediction for the future trajectory and timeline of FFR markets is beyond the scope of this work.

It is evident that the economic viability of an ASG system necessitates a certain set of market tariffs, policies, and regulatory frameworks. The lack of such could act as constraints, barring novel concepts, such as the ASG from implementation

and commercialized use. Illustrated by the results presented in this paper, the operation of the ASG system in the PJM market is only financially profitable with the use of a German standard for DG units that allows the aggregation of downstream DG and the exploitation of their power flexibility without any additional communication infrastructure. This concept would not be feasible within PJM nor in Germany. On the European side, the European Network of Transmission System Operators for Electricity (ENTSO-E) regulatory framework for frequency regulation does not offer a way for smaller and/or fast-acting units to participate in any fast-frequency response service, as PJM offers RegD. The finest granularity for a frequency response service is the Frequency Containment Reserve (FCR), bidding for 4-hour windows [38].

In the case of PJM, the granularity of ancillary markets is much finer, offering 5-minute remuneration windows with signals in a 2-second time resolution. On the American side, on the other hand, the droop-activated regulation does not exist, therefore, whether as an aggregator or a VPP, coordination of behind-the-meter resources without additional communication is hardly feasible at the moment. The aggregation process, as required by regulations such as FERC Order No. 2222, which could be easily and physically attained by operating DGs within clusters of asynchronous grids, as discussed earlier, now necessitates direct communication and interaction with behind-the-meter resources [39]. This diminishes overall performance due to additional delays and decreases the probability of consumer participation if it is an opt-in situation rather than inherently built into behind-the-meter resources. If all aspects are accounted for communication and cloud services for data and edge control management, the economic analysis will be very different, in addition to concerns around cyber-security and data privacy, which are beyond the interest of this paper, but worth noting.

In addition to the fast-frequency response service provision explored in this study, the physical, asynchronous aggregation, and clustering of the power system sections can yield the following advantages:

- Allowing intentional islanding during emergencies and limiting the distance to which a disturbance is propagated.
- Decoupling the grid into smaller clusters and microgrids that can be managed autonomously - with the aim, e.g., to reach net zero emission, net zero power import, or enforce different grid codes.
- The asynchronously connected grid can support the upstream grid - frequency/voltage support [22], [40], [41].
- It can establish demand-side management exploiting voltage and frequency sensitive nodes to offer power flexibility [11], [42], [43].

It is argued that market regulations and tariffs also play a decisive role in the financial mechanism for cost recovery and benefit allocation. In the current American energy market, there are two general ways to recover asset investment capital and network upgrade expenditures. For generation assets, investors recover their costs through revenue in the wholesale market. For reliability assets, e.g., transformers and transmission lines, the investors recover their costs through a guaranteed return rate over a period of time. However, the cost recovery for a ASG system depends on its classification, either as a generation asset, which participates in the ancillary market, or as a reliability asset competing with technologies such as transformers. A third path would be a hybrid model, similar to that of large-scale Energy Storage Systems which are considered Non-wire Alternativ assets. The answer to this question and the extent to which it is allowed to recover from each revenue path lies within the regulations and tariffs of the energy market in which it operates.

On the flip side of revenues and profits, a question looms about the losses and penalties. In addition to the allocation of benefits and compensation to the asset owners and its trickle down to individual household participants, market regulation needs to determine how the losses and disciplinary actions for violations are distributed. Besides the financial losses, the liability and penalties for matters that have an adverse impact on market operations such as defaulting on power, availability commitment, or physical damages need to be determined.

Finally, the importance of socioeconomic aspects of costumers' direct participation in the mechanisms that underlie grid reliability and power market is highlighted. A careful consideration should be given to whether it would succeed through voluntary programs or it should become mandatory. This concern arises from the fact that each consumer is not only the beneficiary of the grid services itself, but also a burden to it. Answering this question falls into the territory of anthropology and sociology, thus, although worth pondering, it is beyond the scope of this paper.

VI. Conclusion

This paper presents an integration study for the recently developed asynchronous grid concept into power systems. The asynchronous grid connection in this study is deployed to physically aggregate distributed generation units, exploiting their local control response to a fundamental grid frequency deviation. This approach eliminates the need for using telecommunication channels. Computer simulations demonstrated the improved dynamic response for a power system as a result of fast power injection by those aggregated resources. The subsequent market analysis shows the economic viability of investment in this technology as the projected revenue well surpasses its capital cost of design and installation, after a maximum of five years. Finally, the critical role of market regulation and tariffs in the adoption of this technology, as the modern grids evolve, is discussed.

Whilst this paper presents a proof of concept, future research could evaluate parallel operation of multiple asynchronous grid connections and their interaction as well as their scalability in larger systems. In addition, a benchmark comparison with competing technologies such as virtual power plants or direct demand side management is needed to further carve out the distinctive characteristics of the proposed concept. Furthermore, studying the interactions between the control systems of this technology and other digital controllers in the system, including inverter-based resources, along with their correlation to the system oscillations, particularly using electromagnetic transient (EMT) models would be interesting.

APPENDIX

TABLE IV: Parameters - AG Support Model.

Parameter	Value	
Frequency Propagation	R	0.02
Load composition	α	1
Proportional Gain Governor	K_{pgov}	421
Integral Gain Governor	K_{igov}	1287
VSM time constant	T_{a}	3.4
VSM Damping	D_{p}	6.6
$f \sim$ P Droop	K_{pf}	0.4

TABLE V: Parameters - Economic Analysis.

Parameter	Symbol	Value
Performance Score	ρ	0.5
Revenue Growth Rate [35]		6 %
O&M Cost (Initial)	c_{OM}	2 % of I
O&M Growth Rate		6 %
Discount Rate [35]	r	6 %
Investment Horizon	T	15 years
Base Investment Cost	I	137.5 $/kVA

TABLE VI: Parameters - 9-Bus Power System Model.

Bus	P (MW)	Q (MW)	Line	R (pu)	X (pu)	Bus Type
1			1-4		0.058	Gen
2	170	5	2-7		0.063	Gen
3	80	-10	3-9		0.057	Gen
4			4-5	0.02	0.920	
5	-120	-50	4-6	0.02	0.920	Load
6	-100	-40	6-9	0.04	0.170	Load
7			5-7	0.035	0.161	
8	-110	-30	7-8	0.08	0.072	Load
9			8-9	0.012	0.101	

ACKNOWLEDGMENT

We wish to thank Enrique Bacalao with the Bacalao Consulting Services, LLC, for his insightful discussions and comments.

This work was supported by the Helmholtz Association under the program "Energy System Design" and the Helmholtz Young Investigator Group "Hybrid Networks" (VH-NG-1613).

This work was authored in part by the National Renewable Energy Laboratory, operated by Alliance for Sustainable Energy, LLC, for the U.S. Department of Energy (DOE) under Contract No. DE AC36-08GO28308. Funding provided by U.S. Department of Energy Office of Energy Efficiency and Renewable Advanced Materials and Manufacturing Technologies Office. The views expressed in the article do not necessarily represent the views of the DOE or the U.S. Government. The U.S. Government retains and the publisher, by accepting the article for publication, acknowledges that the U.S. Government retains a nonexclusive, paid-up, irrevocable, worldwide license to publish or reproduce the published form of this work, or allow others to do so, for U.S. Government purposes.

REFERENCES

[1] IRENA (2023), "World energy transitions outlook 2023: 1.5°C pathway," *International Renewable Energy Agency, Abu Dhabi*, vol. 1, 2023.

[2] IRENA (2020), "Global renewables outlook: Energy transformation 2050," *International Renewable Energy Agency, Abu Dhabi*, 2020.

[3] F. Milano, F. Dörfler, G. Hug, D. J. Hill, and G. Verbič, "Foundations and challenges of low-inertia systems (invited paper)," in *2018 Power Systems Computation Conference (PSCC)*, Jun. 2018, pp. 1–25.

[4] A. Sajadi, R. W. Kenyon, and B.-M. Hodge, "Synchronization in electric power networks with inherent heterogeneity up to 100% inverter-based renewable generation," *Nature communications*, vol. 13, no. 1, p. 2490, 2022.

[5] Lazard Consultant, *Levelized Cost of Energy and Levelized Cost of Storage 2024*, 2024 (accessed August 14, 2024).

[6] A. Sajadi, JP. Ranola, R. W. Kenyon, B.-M. Hodge, and B. Mather, "Electric power industry challenges due to increasing shares of inverter-based resources in power systems," in *2022 IEEE PES Innovative Smart Grid Technologies Conference Europe (ISGT-europe)*. IEEE, 2022, pp. 1–5.

[7] H. Alsharif, M. Jalili, and K. N. Hasan, "Fast frequency response services in low inertia power systems—a review," *Energy Reports*, vol. 9, pp. 228–237, Oct. 2023.

[8] H. Jain, B. Mather, A. K. Jain, and S. F. Baldwin, "Grid-supportive loads—a new approach to increasing renewable energy in power systems," *IEEE Transactions on Smart Grid*, vol. 13, no. 4, pp. 2959–2972, Jul. 2022.

[9] M. S. Misaghian, C. O'Dwyer, and D. Flynn, "Fast frequency response provision from commercial demand response, from scheduling to stability in power systems," *IET Renewable Power Generation*, vol. 16, no. 9, pp. 1908–1924, 2022.

[10] Z. Xu, J. Ostergaard, and M. Togeby, "Demand as frequency controlled reserve," *IEEE Transactions on Power Systems*, vol. 26, no. 3, pp. 1062–1071, Aug. 2011.

[11] Q. Tao, J. Geis-Schroer, F. Wald, M. Courcelle, M. Langwasser, T. Leibfried, M. Liserre, and G. De Carne, "The potential of frequency-based power control in distribution grids," in *2022 IEEE 13th International Symposium on Power Electronics for Distributed Generation Systems (PEDG)*, Jun. 2022, pp. 1–6.

[12] V. Prakash and H. Pandzic, "Fast frequency control service provision from active neighborhoods: Opportunities and challenges," *Electric Power Systems Research*, vol. 217, p. 109161, Apr. 2023.

[13] J. Geis-Schroer, Q. Tao, M. Courcelle, G. Bock, M. Suriyah, T. Leibfried, and G. De Carne, "Power-to-frequency dependency of residential loads in a wider frequency range: An experimental investigation," *IEEE Transactions on Industry Applications*, pp. 1–11, 2024.

[14] Q. Tao, M. Courcelle, J. Geis-Schroer, T. Leibfried, and G. D. Carne, "Experimental investigation of power-to-voltage sensitivity profiles of residential loads for load management studies," *IEEE Transactions on Power Delivery*, pp. 1–12, 2024.

[15] M. Courcelle, Q. Tao, J. Geis-Schroer, T. Leibfried, and G. De Carne, "Perturbation-based load sensitivity identification for solid-state transformer-based load control," *IEEE Transactions on Power Delivery*, pp. 1–12, 2024.

[16] M. Esfahani, A. Alizadeh, B. Cao, I. Kamwa, and M. Xu, "A stochastic-robust aggregation strategy for VPP to participate in the frequency regulation market via backup batteries," *Journal of Energy Storage*, vol. 98, p. 113057, Sep. 2024.

[17] Z. Li, M. Liu, M. Xie, and J. Zhu, "Robust optimization approach with acceleration strategies to aggregate an active distribution system as a virtual power plant," *International Journal of Electrical Power & Energy Systems*, vol. 142, p. 108316, Nov. 2022.

[18] S. Yin, Q. Ai, Z. Li, Y. Zhang, and T. Lu, "Energy management for aggregate prosumers in a virtual power plant: A robust stackelberg game approach," *International Journal of Electrical Power & Energy Systems*, vol. 117, p. 105605, May 2020.

[19] P. Moutis and N. D. Hatziargyriou, "Decision trees-aided active power reduction of a virtual power plant for power system over-frequency mitigation," *IEEE Transactions on Industrial Informatics*, vol. 11, no. 1, pp. 251–261, Feb. 2015.

[20] C. Feng, Q. Chen, Y. Wang, P.-Y. Kong, H. Gao, and S. Chen, "Provision of contingency frequency services for virtual power plants with aggregated models," *IEEE Transactions on Smart Grid*, vol. 14, no. 4, pp. 2798–2811, Jul. 2023.

[21] A. Brooks, E. Lu, D. Reicher, C. Spirakis, and B. Weihl, "Demand dispatch," *IEEE Power and Energy Magazine*, vol. 8, no. 3, pp. 20–29, May 2010.

[22] F. Wald, Q. Tao, and G. De Carne, "Virtual synchronous machine control for asynchronous grid connections," *IEEE Transactions on Power Delivery*, vol. 39, no. 1, pp. 397–406, Feb. 2024.
[23] F. Wald and G. De Carne, "Adaptive virtual synchronous machine control for asynchronous grid connections," in *2023 11th International Conference on Power Electronics and ECCE Asia (ICPE 2023 - ECCE Asia)*, May 2023, pp. 991–996.
[24] P. W. Sauer, J. H. Chow, and M. A. Pai, *Power System Dynamics and Stability: With Synchrophasor Measurement and Power System Toolbox*. Hoboken, NJ, USA: Wiley, 2017.
[25] "Technical rules for the connection of customer installations to the medium-voltage grid and their operation," VDE, Standard VDE-AR-N 4110, Sep. 2023.
[26] "Generating systems on the low-voltage grid minimum technical requirements for the connection and parallel operation of generation systems on the low-voltage grid," VDE, Standard VDE-AR-N 4105, Nov. 2018.
[27] K. Sakimoto, Y. Miura, and T. Ise, "Stabilization of a power system with a distributed generator by a virtual synchronous generator function," in *8th International Conference on Power Electronics - ECCE Asia*, Jan. 2011, pp. 1498–1505.
[28] "Voltage characteristics of public distribution systems," EN 50160, 2020.
[29] Vijay Vittal, James D. McCalley, Paul M. Anderson, and A. A. Fouad, *Power System Control and Stability*. Wiley-IEEE Press, 2020.
[30] A. Sajadi, S. Zhao, K. Clark, and K. A. Loparo, "Small-signal stability analysis of large-scale power systems in response to variability of offshore wind power plants," *IEEE Systems Journal*, vol. 13, no. 3, pp. 3070–3079, Sep. 2019.
[31] A. Fernández Rodríguez, L. de Santiago Rodrigo, E. López Guillén, J. M. Rodríguez Ascariz, J. M. Miguel Jiménez, and L. Boquete, "Coding pronys method in matlab and applying it to biomedical signal filtering," *BMC bioinformatics*, vol. 19, no. 1, p. 451, 2018.
[32] "Final rule order no. 755: Frequency regulation compensation in the organized wholesale power markets," Federal Energy Regulatory Commission, Order 137 FERC 61,064, Oct. 2011.
[33] "PJM - ancillary services," https://www.pjm.com/markets-and-operations/ancillary-services.aspx.
[34] "PJM - data miner 2 - real-time ancillary service market results," https://dataminer2.pjm.com/feed/reserve_market_results.
[35] J. Campos, T. Serebrisky, and A. Suárez-Alemán, "Time goes by: Recent developments on the theory and practice of the discount rate," Inter-American Development Bank, Tech. Rep., Sep. 2015.
[36] J. E. Huber and J. W. Kolar, "Volume/weight/cost comparison of a 1MVA 10 kV/400 V solid-state against a conventional low-frequency distribution transformer," in *2014 IEEE Energy Conversion Congress and Exposition (ECCE)*, Sep. 2014, pp. 4545–4552.
[37] F. Wald, H. V. M., O. Gomis-Bellmunt, H. Ji, M. Davoudi, A. Bidram, M. Syed, M. Josevski, S. Brüske, C. Kumar, R. P. Alzola, I. Colak, S. Pannala, M. Liserre, and G. D. Carne, "Applications and services of solid-state transformers in active distribution networks -a critical review," *IEEE Transactions on Smart Grid*, pp. 1–1, 2025.
[38] D. Fernández-Muñoz, J. I. Pérez-Díaz, I. Guisández, M. Chazarra, and A. Fernández-Espina, "Fast frequency control ancillary services: An international review," *Renewable and Sustainable Energy Reviews*, vol. 120, p. 109662, Mar. 2020.
[39] Federal Energy Regulatory Commission (FERC), "Order no. 2222 - participation of distributed energy resource aggregations in markets operated by regional transmission organizations and independent system operators," Jun. 2021.
[40] D. Shah and M. L. Crow, "Online volt-var control for distribution systems with solid-state transformers," *IEEE Transactions on Power Delivery*, vol. 31, no. 1, pp. 343–350, Feb. 2016.
[41] J. Chen, M. Liu, G. De Carne, R. Zhu, M. Liserre, F. Milano, and T. O'Donnell, "Impact of smart transformer voltage and frequency support in a high renewable penetration system," *Electric Power Systems Research*, vol. 190, Jan. 2021.
[42] Q. Tao, J. Geis-Schroer, M. Courcelle, T. Leibfried, and G. D. Carne, "Investigation of frequency dependency of residential loads in modern power systems: An experimental approach," in *2023 11th International Conference on Power Electronics and ECCE Asia (ICPE 2023 - ECCE Asia)*, May 2023, pp. 329–334.
[43] M. Courcelle, Q. Tao, J. Geis-Schroer, S. Bruno, T. Leibfried, and G. De Carne, "Methods comparison for load sensitivity identification," in *2023 IEEE Belgrade PowerTech*, Jun. 2023, pp. 1–6.

Felix Wald (GS'20) received his bachelor's degree from Berlin University of Applied Sciences in 2019 and his master's degree from the Karlsruhe Institute of Technology in 2021, in electrical engineering. Since February 2021 he is working towards his Ph.D. degree as part of the "Real Time System Integration" group and "Power Hardware-in-the-Loop" lab at the Institute for Technical Physics at the Karlsruhe Institute of Technology, Karlsruhe, Germany. He currently serves as secretary of the IEEE PES Taskforce on "Solid State Transformer Integration in Distribution Grids" and his research interests include Power Hardware-in-the-Loop testing and the technical and economic investigation of power electronic transformers.

Amir Sajadi (S'12, M'16, SM'19) is an Associate Research Professor with the Renewable and Sustainable Energy Institute, University of Colorado Boulder, Boulder, CO, USA, and a Research Affiliate with the National Renewable Energy Laboratory (NREL), Golden, CO, USA. He received the Ph.D. degree in systems and control engineering in 2016 from Case Western Reserve University, Cleveland, OH, USA. His main research interests include modeling, planning, dynamics, control, and management of large-scale power systems to enhance the stability, security, and resiliency of energy delivery.

Barry Mather (SM) received the Ph.D. degree in electrical engineering from the University of Colorado, Boulder, CO in 2010. Since 2010 he has been with the Power Systems Engineering Center at the National Renewable Energy Laboratory in Golden, CO. From 2010 to 2015 he led a project focusing on the technical impacts of the integration of high-penetrations of PV in Southern California Edisons service territory and authored the High-Penetration PV Grid Integration Handbook for Distribution Engineers. He currently leads a group of about 20 researchers focused on power electronics, system-level control, standards, and national- and state-level interconnection issues related to the integration of renewable energy sources at ever higher levels.

Giovanni De Carne (S'14, M'17, SM'21) received the B.Sc. and M.Sc. degrees in electrical engineering from the Polytechnic University of Bari, Italy, in 2011 and 2013, respectively, and the Ph.D. degree from the Chair of Power Electronics, Kiel University, Germany, in 2018. Prof. De Carne is currently full professor at the Institute for Technical Physics at the Karlsruhe Institute of Technology, Karlsruhe, Germany, where he leads the Real Time Systems for Energy Technologies Group and the "Power Hardware In the Loop Lab". He is currently supervising PhD students, managing academic and industrial projects, and developing multi-MW power hardware in the loop testing infrastructures for energy storage systems and hydrogen-based drives. His research interests include power electronics integration in power systems, solid-state transformers, real-time modeling, and power hardware in the loop. He has authored/co-authored more than 100 peer-reviewed scientific papers. His research interests include power electronics integration in power systems, solid-state transformers, real-time modeling, and power hardware in the loop. In October 2023, he successfully hosted the IEEE eGrid2023 Workshop in Karlsruhe with high participation from the industry. He has been the technical program committee chair for several IEEE conferences, and associate editor of the IEEE Transaction on Power Electronics, IEEE Transactions on Power Delivery, IEEE Open Journal of Power Electronics and several other IEEE and IET journals.